Interaction Notes

Note 150

January 1974

NUMERICAL CONSIDERATIONS FOR THE CALCULATION OF CURRENTS INDUCED ON INTERSECTING WIRES USING THE POCKLINGTON INTEGRO-DIFFERENTIAL EQUATION

By

F. M. Tesche
Science Applications, Inc.
P.O. Box 277
Berkeley, California 94701

intersecting wires, calculations, Pocklington integro-differential equation

ABSTRACT

In this note, the method of analyzing the scattering behavior of intersecting wire structures using the Pocklington integro-differential equation is presented. Unlike the often employed Hallén equation, this form of the E-field equation requires no additional boundary conditions on the current in order to get a stable solution. As in previous straight wire studies, it is found that with pulse function expansion and point matching about five zones per half wavelength give an accurate representation of the wire current.

ACKNOWLEDGMENT

I would like to thank Prof. Raj Mittra, Prof. T. Crow, Dr. E.K. Miller, Dr. L. Marin and Dr. T. Shumpert for various discussions regarding this work. Additional thanks are extended to Ms. Claudia Scholz for the manuscript preparation.

This work was supported by Science Applications, Inc. (SAI).

I. Introduction

In attempting to determine the currents and charges induced on aircraft-like structures when exposed to an EMP, it is often common to model the aircraft by a few crossed wires. With such an approximate model, it is then possible to formulate an integral equation for the total current flowing on the wires and solve it using numerical methods. Such a model is valid only at relatively low frequencies, where it can be assumed that only axially directed currents exist on the aircraft. At higher frequencies, it is possible to develop a more complicated integral equation which has as unknowns both orthogonal components of surface current[12], or it is possible to model the aircraft by a number of interconnected wires forming a mesh[11].

In both the wire mesh and the crossed wire models it is important to insure that the numerical method employed for the solution provides the correct behavior of the currents and charges at wire junctions. A number of investigators[3,4,5,6,7,13,14,15] have looked at the junction problem in the past. However, the majority of such research has been

related to the Hallén form of the E-field integral equation, which requires that specific boundary conditions be imposed on the wire currents in order to obtain a unique solution.

It is well known that the Pocklington form of the E-field equation gives results which are almost identical to those of Hallén's equation for a single straight or curved wire[10]. This is done, moreover, without making use of explicit boundary conditions for the current. As will be seen shortly, the same is true for intersecting wires which are treated by the Pocklington equation. The computed values of current at wire end points and at the junctions can then be used to determine the accuracy of the overall solution, since their behavior at these points is already known from Kirchoff's law and charge conservation.

There is more than just academic interest to warrant further studies of the junction problem. Since the ultimate goal is to obtain the frequency domain and corresponding time domain behavior of the induced charge and current on the aircraft structure, it is necessary to have a computer code which is efficient and rapidly converging. This is true not only if conventional FFT methods[2,15] are used to compute the transient response, but also if SEM[1,17] is used. Because the vector potential $\bar{A}$ is not oriented in a single direction for a general collection of interesting wires, the Hallén form of the E-field equation

becomes tedious to program and time consuming to run on the computer. The Pocklington equation, on the other hand, is much easier to program and runs relatively rapidly on the computer.

In this note, therefore, a brief study of the application of Pocklington's equation to intersecting thin-wire structures is presented. It is found that remarkable convergence is obtained, but that a certain degree of consistency must be maintained in numerically performing the integrations and differentiations required in the process of obtaining a solution. The interesting question of how thick cylinders behave is not treated here, but certainly deserves additional study, with special emphasis on the junction.

II. Formulation

The starting point for formulating the Pocklington integral equation for a scatterer is Maxwell's equations[20]. From these it is a well known fact that the $\bar{E}$ and $\bar{H}$ fields can be represented by potentials $\bar{A}$ and ϕ in the following manner:

$$\bar{E}(\bar{r}_o) = -j\omega\bar{A}(\bar{r}_o) - \nabla_o\phi(\bar{r}_o) \tag{1a}$$

$$\bar{H}(r_o) = \mu_o^{-1}\nabla_o\times\bar{A}(\bar{r}_o) \tag{1b}$$

where $\bar{r}_o$ is an arbitrary observation point shown in Figure 1. A time dependence of $e^{j\omega t}$ is assumed and suppressed.

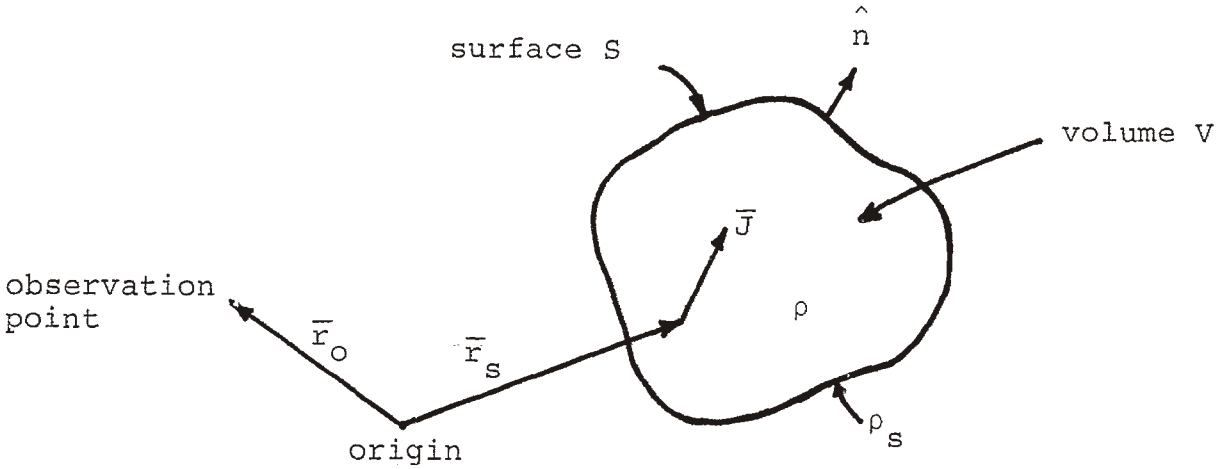

Figure 1.

The potentials $\bar{A}$ and ϕ are related to the current density $\bar{J}$ and charge density ρ which exist in the region where the fields are to be computed, and are expressed as

$$\bar{A}(\bar{r}_o) = \mu_o \int_{\text{sources}} \bar{J}(\bar{r}_s)\, G(\bar{r}_o, \bar{r}_s)\, dV_s \qquad (2a)$$

and

$$\phi(\bar{r}_o) = \frac{1}{\varepsilon_o} \int_{\text{sources}} \rho(\bar{r}_s)\, G(\bar{r}_o, \bar{r}_s)\, dV_s \quad , \qquad (2b)$$

where Green's function $G(\bar{r}_o, \bar{r}_s)$ is a solution to

$$\nabla^2 G + k^2 G = \delta(\bar{r}_o - \bar{r}_s) \qquad (3)$$

and has the form

$$G(\bar{r}_o, \bar{r}_s) = \frac{e^{-jk|\bar{r}_o - \bar{r}_s|}}{4\pi|\bar{r}_o - \bar{r}_s|} \quad . \qquad (4)$$

It is now possible to insert (2a) and (2b) into (1a) to determine the electric field produced by the current and charge in the volume V. In typical electromagnetic scattering problems, however, these quantities are induced by the incident field and must be calculated. Instead of determining $\bar{J}$ and ρ together, it is possible to use the

$\nabla\times\overline{H}$ Maxwell equation and derive the continuity equation, which is

$$\nabla\cdot\overline{J} = -j\omega\rho \quad . \tag{5}$$

In addition to the volume charge density ρ, it is possible to have a surface charge density[20], given by ρ_s, which satisfies

$$j\omega\rho_s = \hat{n}\cdot\overline{J} \tag{6}$$

where $\hat{n}$ is the outward normal from the surface S which encloses the sources of charge and currents, as shown in Figure 1.

With these relations, the electric field produced by the currents and charges within the volume V may then be expressed as:

$$\overline{E}(\overline{r}_o) = -j\omega\mu_o \int_V \overline{J}(\overline{r}_s)\ G(\overline{r}_o,\overline{r}_s)\ dV_s$$

$$+ \frac{1}{j\omega\varepsilon_o}\nabla_o\left[\int_V \nabla_s\cdot\overline{J}(\overline{r}_s)G(\overline{r}_o,\overline{r}_s)dV_s - \int_S \hat{n}\cdot\overline{J}(\overline{r}_s)G(\overline{r}_o,\overline{r}_s)dS_s\right] . \tag{7}$$

For an isolated body which lies completely within a sphere of some finite radius, it is known that the normal surface current is zero. Thus, the last term in Eq. (7) can be omitted. However, if Eq. (7) is applied to only part of a current carrying conductor, it is necessary to retain this term.

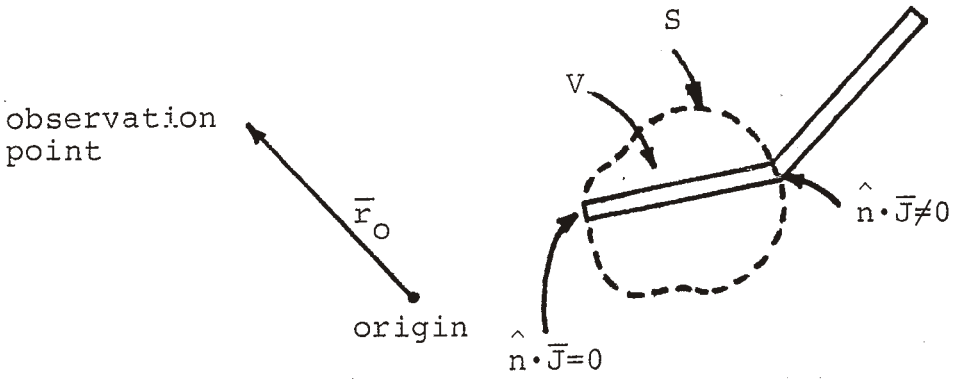

Figure 2.

Consider the example of two intersecting wires shown in Figure 2, where it is desired to compute the $\bar{E}$ field at $\bar{r}_o$, assuming that the currents $\bar{J}$ on the wires 1 and 2 are known. If the entire structure is considered, the integral over S vanishes since $\hat{n}\cdot\bar{J} = 0$ at the ends of the current carrying region. However, if only wire 1 is considered, $\hat{n}\cdot\bar{J} \neq 0$ at the end near the junction, implying that the additional term in Eq. (7) must be retained. However, the total field at $\bar{r}_o$ is produced by currents on wire 1 and wire 2, and it is easy to show that the contribution from

$\hat{n}\cdot\bar{J}$ on wire 1 cancels that of $\hat{n}\cdot\bar{J}$ of wire 2, provided that the current flow is continuous across the junction. This implies that if Kirchoff's current law holds at the wire junction, the surface integral in Eq. (7) need not be included if Eq. (7) is applied to each separate leg of the wire scatterer and the results then summed to get the total field. This result is easily extendable to an arbitrary number of intersecting wires.

Instead of invoking Kirchoff's law and setting the last term of Eq. (7) to zero, however, Eq. (7) can be simplified by noting that for a scalar function ϕ and a vector function $\bar{a}$

$$\nabla(\phi\bar{a}) = (\nabla\cdot\bar{a})\phi + \nabla\phi\cdot\bar{a} \quad . \tag{8}$$

Integrating this over a volume V and using the divergence theorem yields

$$\int_V (\nabla\cdot\bar{a})\phi \, dV = \int_S \hat{n}\cdot\bar{a} \, \phi ds - \int_V \nabla\phi\cdot\bar{a} \, dV \quad . \tag{9}$$

Letting $\bar{a} = \bar{J}$ and $\phi = G$, and applying Eq. (9) to Eq. (7), it is possible to transfer the ∇_s operation from the current over to Green's function, as well as eliminate the integral over the surface S. Thus, Eq. (7) becomes

$$\bar{E}(\bar{r}_o) = -j\omega\mu_o \int_V \bar{J}(\bar{r}_s)\, G(\bar{r}_o, \bar{r}_s)\, dV_s$$

$$- \frac{1}{j\omega\varepsilon_o} \nabla_o \int_V \bar{J}(\bar{r}_s)\cdot\nabla_s\, G(\bar{r}_o, \bar{r}_s)\, dV_s \quad . \quad (10)$$

Note that Eq. (10) involves only the current densities $\bar{J}$, without added boundary conditions. This equation is valid for the whole current carrying volume, or just a portion of it. If it is used to form an integral equation for the unknown currents $\bar{J}$, the fact that Kirchoff's current law must be obeyed at any junction is inherent in the equation.

The integral equation for the unknown current $\bar{J}$ is formed by letting the observation point $\bar{r}_o$ approach the volume of current and then relating the scattered field to the incident field. Note that the integrand in Eq. (10) becomes singular as $\bar{r}_o \Rightarrow \bar{r}_s$. The highest order singularity is of the form $1/r^2$ which is integrable within a volume V. If only surface currents are considered, as in the case of a perfectly conducting body, this integral is still integrable. In many cases it is tempting to put the ∇_o operation within the integral of the last portion of Eq. (10), yielding

$$\bar{E}(\bar{r}_o) = -\frac{1}{j\omega\varepsilon_o}\int_V \left[\bar{J}(\bar{r}_s)\cdot\nabla_o\right]\nabla_s G(\bar{r}_o,\bar{r}_s) - k^2\bar{J}\,G(\bar{r}_o,\bar{r}_s)\,dV_s \tag{11}$$

Noting that $\nabla_s G = -\nabla_o G$, Eq. (11) is written commonly as

$$\bar{E}(\bar{r}_o) = +\frac{1}{j\omega\varepsilon_o}\int \bar{J}(\bar{r}_s)\cdot\underline{\underline{\Gamma}}(\bar{r}_o,\bar{r}_s)\,dV_s \tag{12}$$

where the dyadic Green's tensor $\underline{\underline{\Gamma}}$ is defined as

$$\underline{\underline{\Gamma}}(\bar{r}_o,\bar{r}_s) = (\nabla_o\nabla_o + k^2\underline{\underline{I}})\,\frac{e^{-jk|r_o-r_s|}}{4\pi|\bar{r}_o-\bar{r}_s|} \tag{13}$$

If Eq. (12) is employed to form an integral equation by letting $\bar{r}_o$ approach $\bar{r}_s$, it is seen that the integrand now has a $1/r^3$ singularity which is non-integrable. The process of simply interchanging the operation ∇_o and the integration is valid for points where $\bar{r}_o \neq \bar{r}_s$. The treatment of the case when $r_o=r_s$ has been discussed by Van Bladel[21], and involves taking the principal value of the integral in Eq. (12), as well as adding an extra term $J/3j\omega\varepsilon$ for the singular contribution. For the present study, however, the less singular Eq. (10) will be employed to form the integral equation.

For a thin, intersecting wire scatterer it is possible to make a number of simplifications in Eq. (10) in order to derive the integral equation. By assuming that only the total axial currents and fields are important and using the condition $(\bar{E}^{inc} + \bar{E}^{sca})_{tan} = 0$ on the wires, Eq. (10)

yields the following integral equation

$$-j\omega\varepsilon_o E_{tan}^{inc}(\bar{\xi}_o) = k^2 \int_L I(\bar{\xi}_s) K(\bar{\xi}_o, \bar{\xi}_s) \hat{\xi}_o \cdot \hat{\xi}_s d\bar{\xi}_s$$

$$- \frac{\partial}{\partial \xi_o} \int_L I(\bar{\xi}_s) \frac{\partial K}{\partial \xi_s} d\bar{\xi}_s \quad , \qquad (14a)$$

where $\bar{\xi}_o$ and $\bar{\xi}_s$ are the distances from the junction to the observation and source points, and the kernel K is related to the integral of G around the wire circumference and is given approximately by

$$K(\bar{\xi}_o, \bar{\xi}_s) = \frac{e^{-jk\sqrt{(\bar{\xi}_o - \bar{\xi}_s)^2 + a^2}}}{4\pi\sqrt{(\bar{\xi}_o - \bar{\xi}_s)^2 + a^2}} \qquad (14b)$$

for thin wires[10]. In this equation, there are derivatives on both the source and observation points, due to the fact that the direction of the current flow is not always the same on the wire structure. If this were the case, as in a straight wire antenna, Eq. (14a) reduces to the well-known equation[17].

$$-j\omega\varepsilon_o E_{tan}^{inc}(\bar{\xi}_o) = \left(k^2 + \frac{d^2}{d\xi_o^2}\right) \int I(\bar{\xi}_s) \; K(\bar{\xi}_o, \bar{\xi}_s) d\bar{\xi}_s \; . \qquad (15)$$

III. Numerical Technique

The solution of Eq. (14a) is effected by using the moment method[9]. The expansion functions for the current will be chosen to be pulse functions and the testing functions are delta functions which implies a point-match solution. Previous experience with the solution of Pocklington's equation in this manner has shown that these choices lead to a reasonably rapidly converging and stable solution for the current[16,17].

Instead of carrying out the derivative $\frac{\partial}{\partial \xi_s}$ in Eq. (14a) explicitly, experience has shown that a finite difference method for evaluating this quantity gives good results.

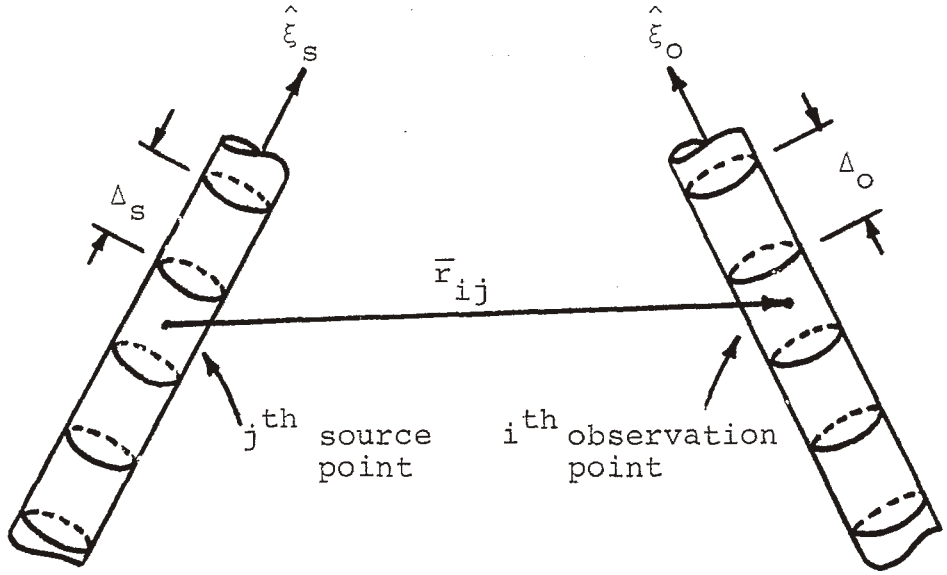

Figure 3.

The same holds for the $\frac{\partial}{\partial \xi_o}$ operation. Consider the two, nonparallel wire segments shown in Figure 3, each of which is divided into a number of cells of length Δ in which the induced current is assumed constant. For the i^{th} observation point, and the j^{th} source point, the matrix element Z_{ij} is given by

$$Z_{i,j} = \frac{j\Delta_s}{\omega\varepsilon_o}\left\{\int_{\xi_j-\frac{\Delta_s}{2}}^{\xi_j+\frac{\Delta_s}{2}} K(\xi_i,\xi)\hat{\xi}_i\cdot\hat{\xi}\ d\xi\right.$$

$$-\frac{1}{\Delta_o}\left[\int_{\xi_j-\frac{\Delta_s}{2}}^{\xi_j+\frac{\Delta_s}{2}} \frac{K\left(\xi_i+\frac{\Delta_o}{2},\xi+\frac{\Delta_s}{2}\right) - \left(K\ \xi_i+\frac{\Delta_o}{2},\xi-\frac{\Delta_s}{2}\right)d\xi}{\Delta_s}\right.$$

$$\left.\left.-\int_{\xi_j-\frac{\Delta_s}{2}}^{\xi_j+\frac{\Delta_s}{2}} \frac{K\left(\xi_i-\frac{\Delta_o}{2},\xi+\frac{\Delta_s}{2}\right) - \left(K\ \xi_i-\frac{\Delta_o}{2},\xi-\frac{\Delta_s}{2}\right)d\xi}{\Delta_s}\right]\right\} \quad (16)$$

where ξ_{s_j} and ξ_{o_i} have been defined simply as ξ_j and ξ_i. Note that in these equations, a center finite difference scheme has been used with sample points a distance of $\pm\Delta$ away from the ξ_i and ξ_j points.

By denoting each of the separate integrated kernel terms in Eq. (10) by $\Phi_{i,j}$, $\Phi_{i+,j+}$, etc., Eq. (16) takes the following form

$$Z_{ij} = \frac{j\Delta_s}{\omega\varepsilon_o}\left\{\Phi_{i,j} - \frac{1}{\Delta_o\Delta_s}\left[\Phi_{i+,j+} - \Phi_{i+,j-} - \Phi_{i-,j+} + \Phi_{i-,j-}\right]\right\} . \tag{17}$$

Because the kernel K is non-singular, due to the thin-wire approximation given by Eq. (14b), the values of Φ are readily determined by direct machine integration.

It is interesting to note that the above finite difference expression is identical with that which would be obtained if Eq. (11) were to be used, since $\bar{r}_o \neq \bar{r}_s$. For the case when ξ_s and ξ_o are at the same cross section of the same wire, Eq. (17) will give the correct value for the impedance matrix because the integration is performed before the differentiation is carried out by the finite difference method.

The method of zoning the scatterer near the ends of a wire and in the vicinity of a junction is illustrated in Figure 4. Near the end of the wire a sample point is located such that it lies exactly at the end of the wire[9]. Denoted by i = 0, it is easy to show that the current in this cell can contribute one row and column to the system impedance matrix Z. However, if one uses the a priori knowledge that

I = 0 at the wire end, it is possible to completely eliminate these contributions to the matrix, thereby requiring only cells 1, 2, 3, etc.

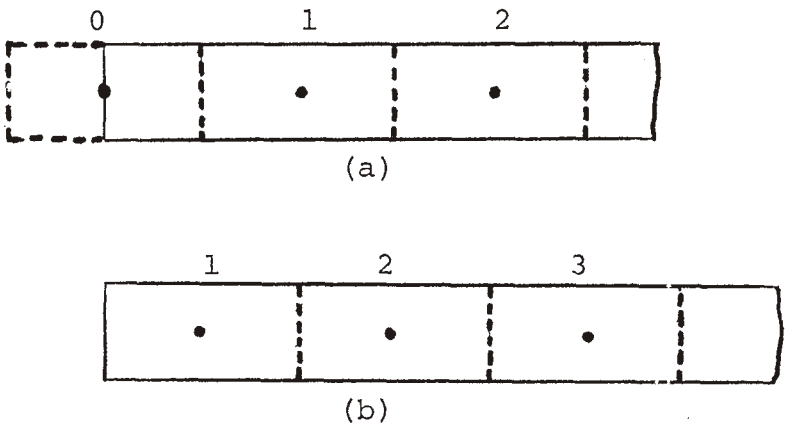

Figure 4.

Another way of treating the end, however, is shown in Figure 4b where the zoning of the wire starts exactly from the end of the wire. This method also gives good results, although they are slightly different from those obtained using the previous zoning method. The reason is that by using pulse functions the actual length of the scatterer is ambiguous to within a factor on the order of the size of the cell Δ. Thus, as Δ becomes smaller, the results of (a) and (b) in Figure 4 tend to converge as long as all integrations and other numerical procedures are done consistently.

The method of zoning at the wire junction is shown in Figure 5. At the junction, the first cell starts right at the end of the wire without a half-zone overlap. Note that there is a small portion of each zone which overlaps adjacent zones. For thin structures, this overlap appears to be of no consequence, but as the radius of the wire approaches the cell width, appreciable errors may be present. The treatment of such problems still needs to be considered.

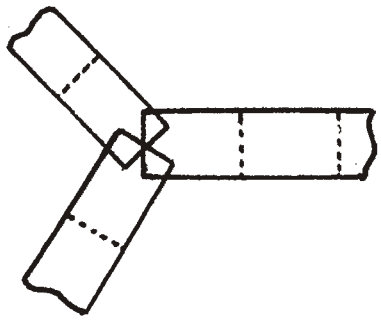

Figure 5. Zoning at the wire junction

There has been some concern expressed that, for the types of zoning illustrated in Figures 4b and 5, the sample points used for taking the finite differences to approximate the derivatives in Eq. (14a) can lie outside the metallic boundary of the conductor. This concern may be justified if such operations were to operate on the current, as in Eq. (7), but in the present case all that one is interested in is the variation of the kernel

in space. Whether there is metal near one of the finite difference points or not is unimportant. What is important, however, is that the eventual matching point be located on the metal so as to permit the enforcing of the proper boundary condition at that point.

With these considerations, the resulting matrix equation for the unknown current takes the form

$$[Z][I] = [V] \tag{18}$$

where the vector $[V]$ represents the voltage drop of the incident field across each cell and is given by

$$V_j = E^{inc}(\xi_j)\ \Delta_j \tag{19}$$

for a point match solution. The solution for the current is then obtained using standard matrix inversion algorithms.

IV. Computation Results and Discussion

To study the behavior of this particular formulation of the E-field equation when applied to intersecting wire structures, the planar, three-arm scatterer shown in Figure 6 was investigated in some detail. In the computations, no knowledge regarding the behavior of the currents at the junctions was included in the solution, although the fact that I = 0 at the wire ends was used implicitly by choosing the zoning illustrated in Figure 4a.

It is of some interest to compare the solutions obtained for various sampling densities of the current. Figure 7 shows both the real and imaginary parts of the induced current on legs 1, 2, and 3 of the scatterer having the parameters $L_1 = L_2 = L_3 = .5\lambda$, $\theta_1 = 90^\circ$, $\theta_2 = 120^\circ$, $\Omega = 2 \ln(L_1/a) = 10$ $(a=.0034\lambda)$. From this figure it is seen that the convergence of the solution as a function of the number of sample points on each leg is remarkably good. Even for three sample points on each leg of the structure, the current values are reasonably accurate. The trouble with using only three points, however, is that it is difficult to interpolate the current values between the known points. Thus, a higher number of sample points must usually be used.

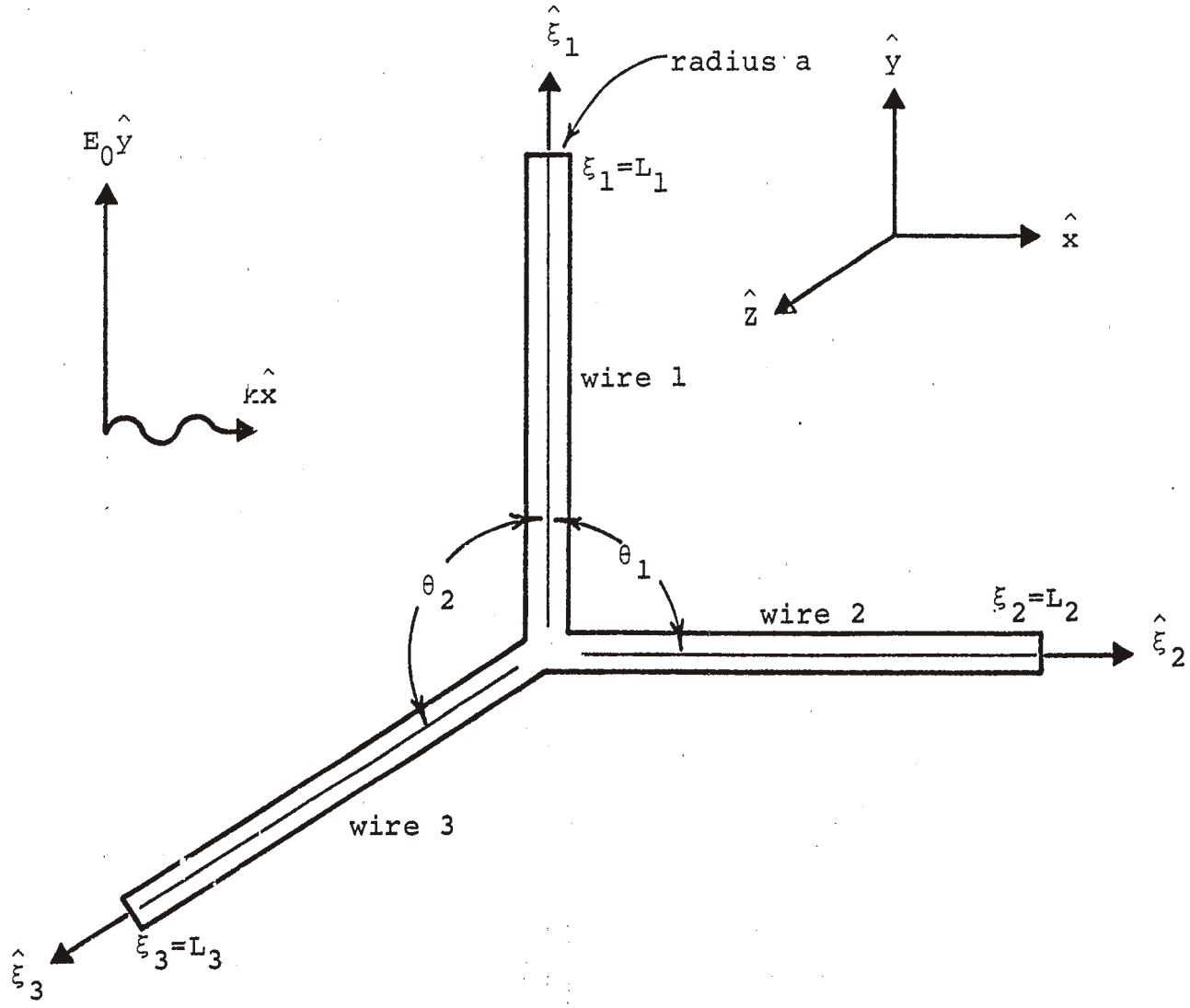

Figure 6. Geometry of a planar, three-arm scatterer.

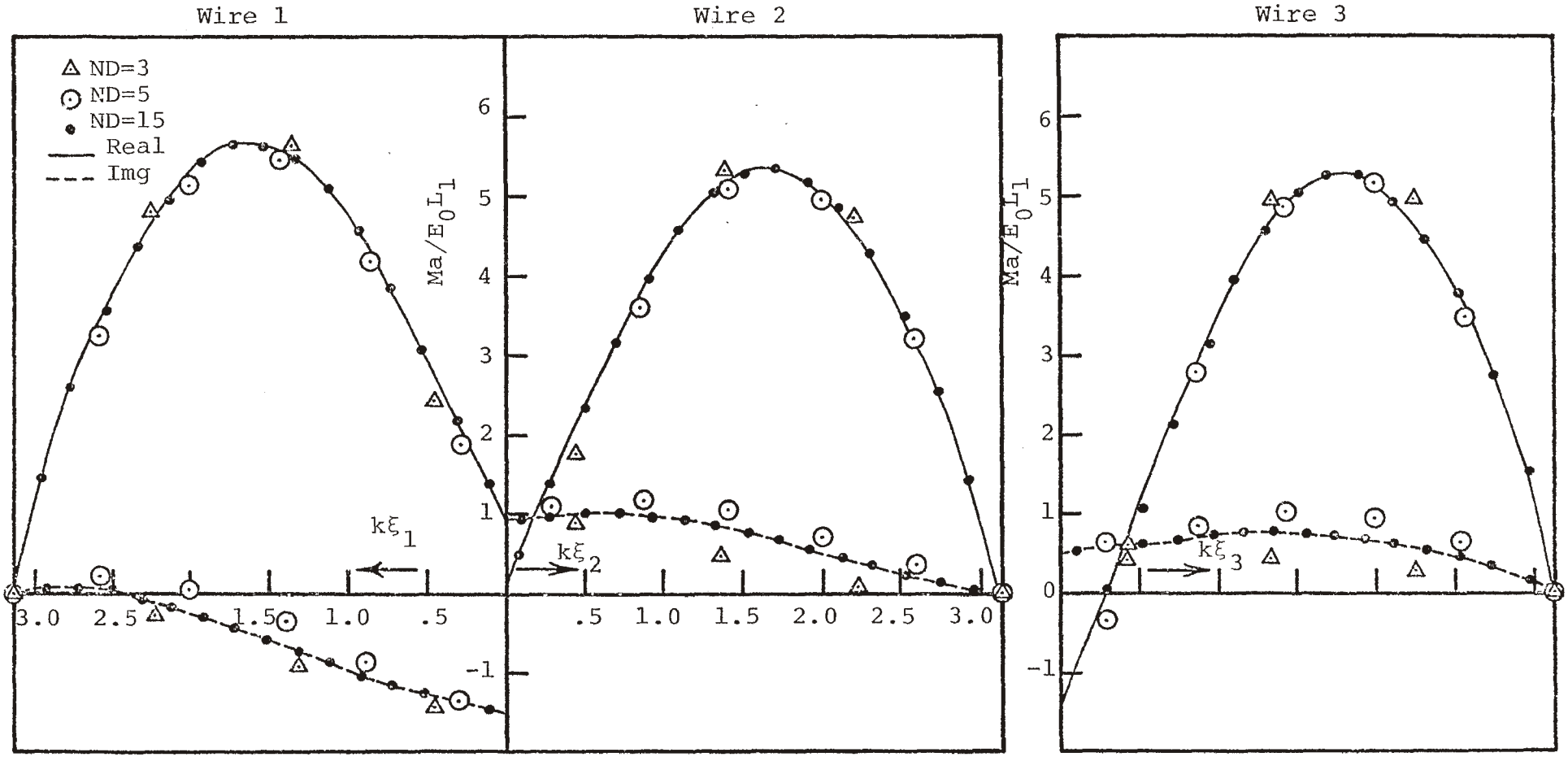

Figure 7. Currents induced on three intersecting wires with $L_1=L_2=L_3=.5\lambda$, $\theta_1=90^\circ$, $\theta_2=120^\circ$, $\Omega=2\ell n(L_1/a)=10.$, shown for various values of ND, the number of sampling points per wire.

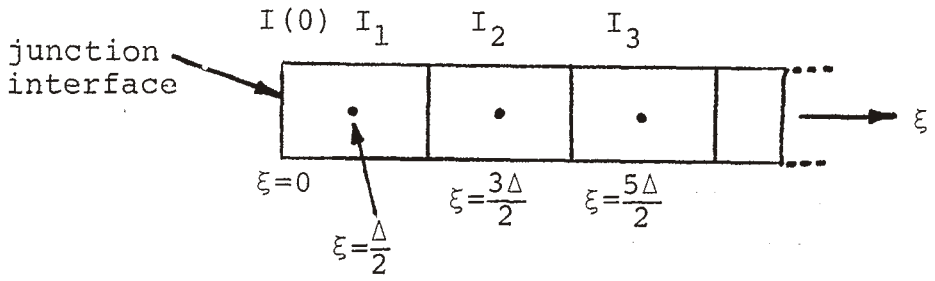

Figure 8.

In Figure 7 it is noted that the currents are assumed to be positive when flowing away from the junction. One estimate of the accuracy of the solution is to look at Kirchoff's current law at the junction. Since the current is not known exactly at the junction, it is necessary to extrapolate its value from previously determined values. Consider Figure 8 which shows the first three cells on a particular wire. The current on the wire can be expanded in a Taylor series as

$$I(\xi) = I(0) + I'(0)\xi + \frac{I''(0)}{2}\xi^2 + \ldots \quad . \qquad (20)$$

By keeping the first three terms and equating to I_1 , I_2 and I_3 at $\Delta/2$, $3\Delta/2$ and $5\Delta/2$ respectively, the following equation results

$$\begin{bmatrix} 1 & \frac{\Delta}{2} & \frac{\Delta^2}{8} \\ 1 & \frac{3\Delta}{2} & \frac{9\Delta^2}{8} \\ 1 & \frac{5\Delta}{2} & \frac{25\Delta^2}{8} \end{bmatrix} \begin{bmatrix} I(0) \\ I'(0) \\ I''(0) \end{bmatrix} = \begin{bmatrix} I_1 \\ I_2 \\ I_3 \end{bmatrix} \qquad (21)$$

which can be solved for I(0). This gives the extrapolated junction current as

$$I(0) = \frac{15I_1 - 10I_2 + 3I_3}{8} \quad . \qquad (22)$$

The junction currents for each wire have been computed by this method and then summed to verify Kirchoff's law. Figure 9 shows the magnitude of the sum of the junction currents expressed as a percentage of the magnitude of the largest current value found on the scatterer after numerical convergence has been obtained. It is noted that for three sample points on each wire, the error in Kirchoff's law is as large as the maximum value of the current, while the error drops to 10% for fifteen points per leg.

It is a bit puzzling to have such large discrepancies in the junction current sum when the calculated values of the wire currents appear to be fairly independent of the number of sample points, as witnessed by Figure 7. The

answer lies in the uncertainty inherent in the extrapolation process. For only three sample points on a particular wire, it is not reasonable to expect that the three-point formula for the junction current of Eq. (22) will give accurate results.

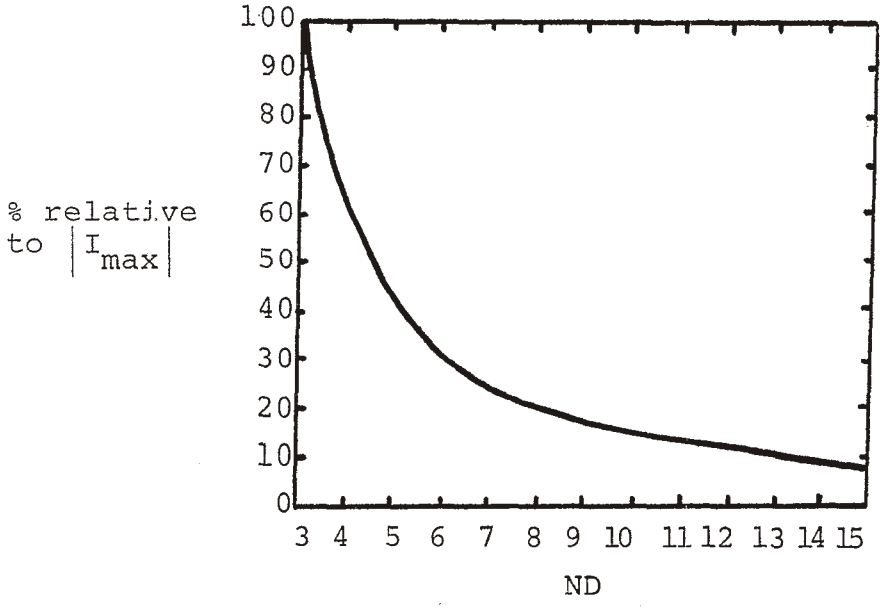

Figure 9. Error in Kirchoff's current law at junction as a function of the number of sample points, ND.

One solution to this problem is to simply take more sample points and then the extrapolated solution for the junction current becomes closer and closer to the exact solution. In many instances, however, this procedure is not desirable due to the need to keep computer time at a minimum. Moreover, as the number of cells increases, the Δ/a ratio decreases and eventually the thin wire approximation becomes invalid.

A possible way to overcome this difficulty is to determine the junction currents from the wire currents using the knowledge of Kirchoff's law at the junction. Consider three intersecting wires, each assumed to have the same radius. The currents on each are labeled as $I(\xi)$, $J(\xi)$ and $K(\xi)$ respectively. As done previously, each current can be expanded in a Taylor series of the form

$$I(\xi_1) = I(0) + C_1\xi_1 + C_2\xi_1^2$$

$$J(\xi_2) = J(0) + C_3\xi_2 + C_4\xi_2^2 \qquad (23)$$

$$K(\xi_3) = K(0) + C_5\xi_3 + C_6\xi_3^2$$

where C_1 , C_2 , C_3 , C_4 , C_5 and C_6 are unknown, as well as are the junction currents.

To find these values, it is possible to equate Eqs. (23) to the appropriate values I_1, I_2, J_1 , J_2 , K_1 and K_2 , giving six equations in nine unknowns. Another independent equation is found from the Kirchoff current law

$$I(0) + J(0) + K(0) = 0 \quad . \qquad (24)$$

The final equations come from the derivatives of the current at the junction. The surface charge at any point on the wire is given from the continuity equation as

$$\rho_s = -\frac{1}{j\omega} \nabla \cdot \bar{J} \tag{25}$$

where $\bar{J}$ is the current density on the surface of the wire. Since $\bar{J}$ is in the $\hat{\xi}$ direction only and is independent of the circumferential direction, it's related to the total current by $\bar{J} = I(\xi)\ \hat{\xi}/2\pi a$, where a is the wire radius. Thus, Eq. (25) for the surface charge density on the wire becomes

$$\rho_s = -\frac{1}{j\omega} \frac{1}{2\pi a} \frac{dI(\xi)}{d\xi} \quad . \tag{26}$$

The physical argument that the surface charge density approaches the same value as an observer moves along a wire towards the junction regardless of which wire he is on provides the additional equations

$$\frac{I'(0)}{a_I} = \frac{J'(0)}{a_J} = \frac{K'(0)}{a_K} \tag{27}$$

where a_I, a_J and a_K are the radii of the wires and the symbol $'$ represents the derivative in the direction of the wire.

Thus, from Eq. (23) it is seen that the constants C_1 , C_3 and C_5 are related as

$$C_3 = \frac{a_I}{a_J} C_1$$

$$C_5 = \frac{a_I}{a_K} C_1 \quad . \tag{28}$$

Collecting these equations together, they may be expressed in matrix form as

$$\begin{bmatrix} 1 & 0 & 0 & \frac{\Delta}{2a_I} & \frac{\Delta^2}{4} & 0 & 0 \\ 1 & 0 & 0 & \frac{3\Delta}{2a_I} & \frac{9\Delta^2}{4} & 0 & 0 \\ 0 & 1 & 0 & \frac{\Delta}{2a_J} & 0 & \frac{\Delta^2}{4} & 0 \\ 0 & 1 & 0 & \frac{3\Delta}{2a_J} & 0 & \frac{9\Delta^2}{4} & 0 \\ 0 & 0 & 1 & \frac{\Delta}{2a_K} & 0 & 0 & \frac{\Delta^2}{4} \\ 0 & 0 & 1 & \frac{3\Delta}{2a_K} & 0 & 0 & \frac{9\Delta^2}{4} \\ 1 & 1 & 1 & 0 & 0 & 0 & 0 \end{bmatrix} \begin{bmatrix} I(0) \\ J(0) \\ K(0) \\ C_1 \\ C_2 \\ C_4 \\ C_6 \end{bmatrix} = \begin{bmatrix} I_1 \\ I_2 \\ J_1 \\ J_2 \\ K_1 \\ K_2 \\ 0 \end{bmatrix} \tag{29}$$

This may be solved and used to determine adjusted values for the junction currents I(0), J(0) and K(0).

Figure 10 shows the interpolated values of the magnitudes of the junction currents as well as the adjusted values using the above technique for the same structure as treated in Figure 7. Note that as the number of sample points increases, the interpolated and the adjusted currents begin to converge, indicating consistency in the treatment of the currents. Moreover, the adjusted values are very stable as a function of ND, the number of samples. Thus, with only five or six samples on each wire, good current distributions can be obtained. Note also that Kirchoff's current law is now obeyed exactly by the extrapolated junction currents.

A further test of the validity of the numerical solution is to look at the surface charge density along the wire scatterer. In the present case, where the radii of each arm are equal, it is sufficient to plot $\partial I/\partial \xi$ as done in Figure 11. This was obtained by taking finite differences of the current I, once it was computed from the integral equation (14a). Note that at the junction the slopes are very nearly equal, indicating good accuracy in the numerical solution.

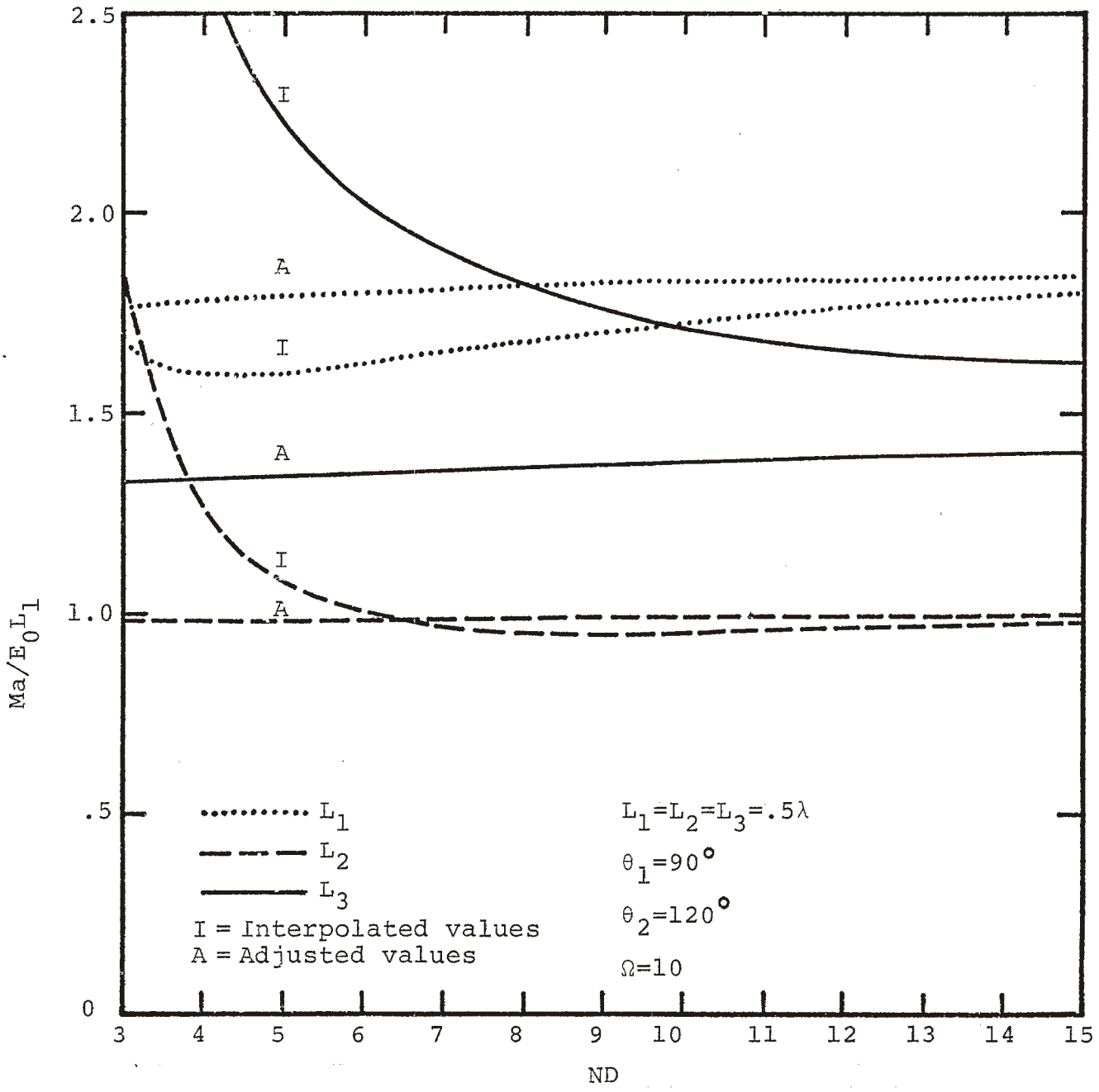

Figure 10. Plots of the magnitude of the junction currents on L_1, L_2 and L_3 as a function of the number of sample zones, ND.

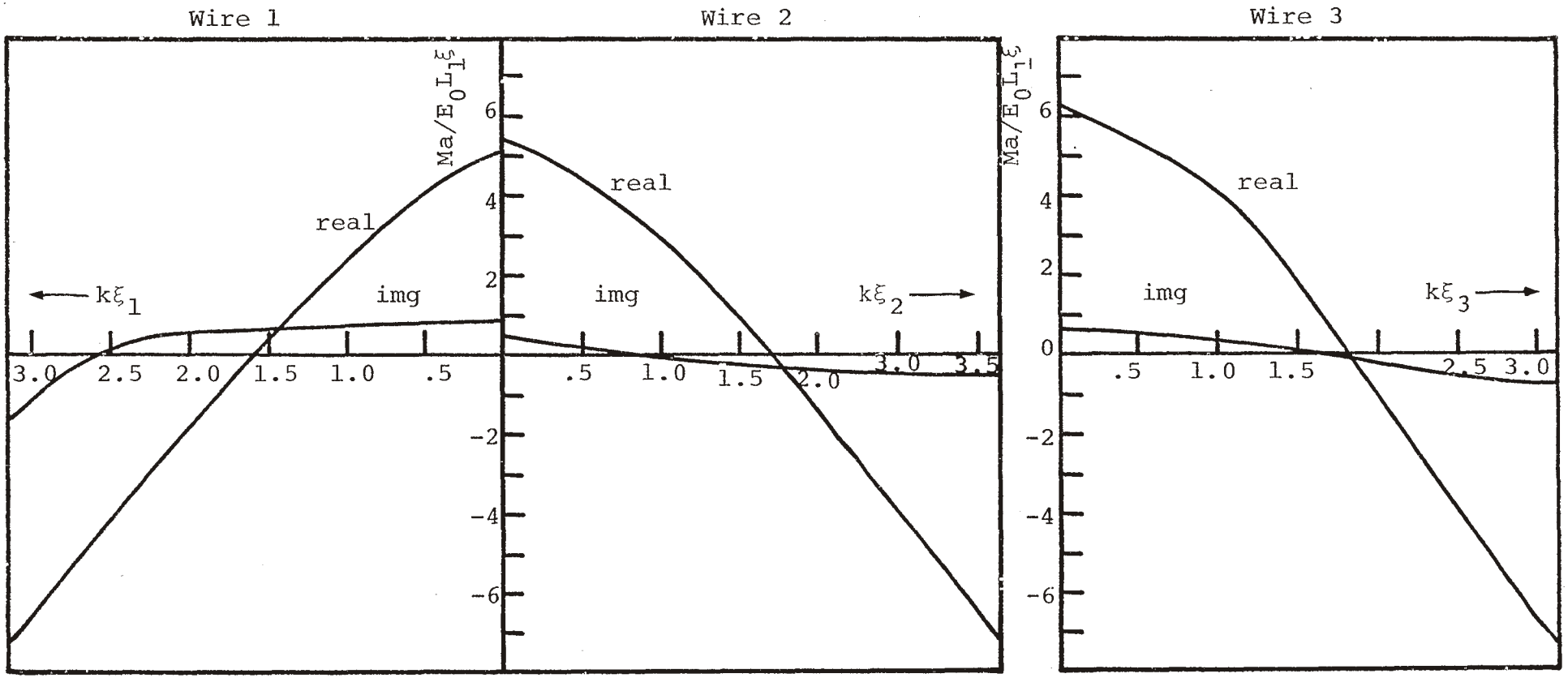

Figure 11. Plots of the slope of the currents ($dI/d\xi$) at the junction of each wire. $L_1=L_2=L_3=.5\lambda$, $\theta_1=90^\circ$, $\theta_2=120^\circ$, $\Omega=2\ell n(L_1/a)=10$.

In Figure 12, the computed results for an inverted T structure are presented for various lengths of the cross members L_1 and L_2 (see diagram on Figure 12). In this case, $L_1 = .5\lambda$, $\theta_1 = \theta_2 = 90^\circ$, $\Omega = 2 \ln(L_1/a) = 10$ and $L_2 = L_3$ varies from $.071\lambda$ to $.5\lambda$. Near the points where L_2 and $L_3 = 0$, the L_1 member resonates at its first natural resonance and the currents increase in magnitude dramatically. In addition, another resonance is apparent near the point where L_2 and L_3 approach $.5\lambda$ as the induced currents again become larger.

Some final remarks are in order regarding the numerical difficulties encountered in solving Pocklington's equation for structures with junctions. The whole reason for using a finite difference scheme for evaluating the matrix elements in Eq. (17) was to eliminate the need to integrate highly singular integrands. If the source point is distant from the observation point, it is then permissible to express the matrix element as the E-field radiated by a current element of moment $I\Delta$. The fields produced by such a current element are given[8] as

$$E_r = \frac{I\Delta}{2\pi} e^{-jkr} \left(\frac{Z_o}{r^2} + \frac{1}{j\omega\varepsilon r^3} \right) \cos\theta$$

$$E_\theta = \frac{I\Delta}{4\pi} e^{-jkr} \left(\frac{j\omega\mu}{r} + \frac{Z_o}{r^2} + \frac{1}{j\omega\varepsilon r^3} \right) \sin\theta \qquad (30)$$

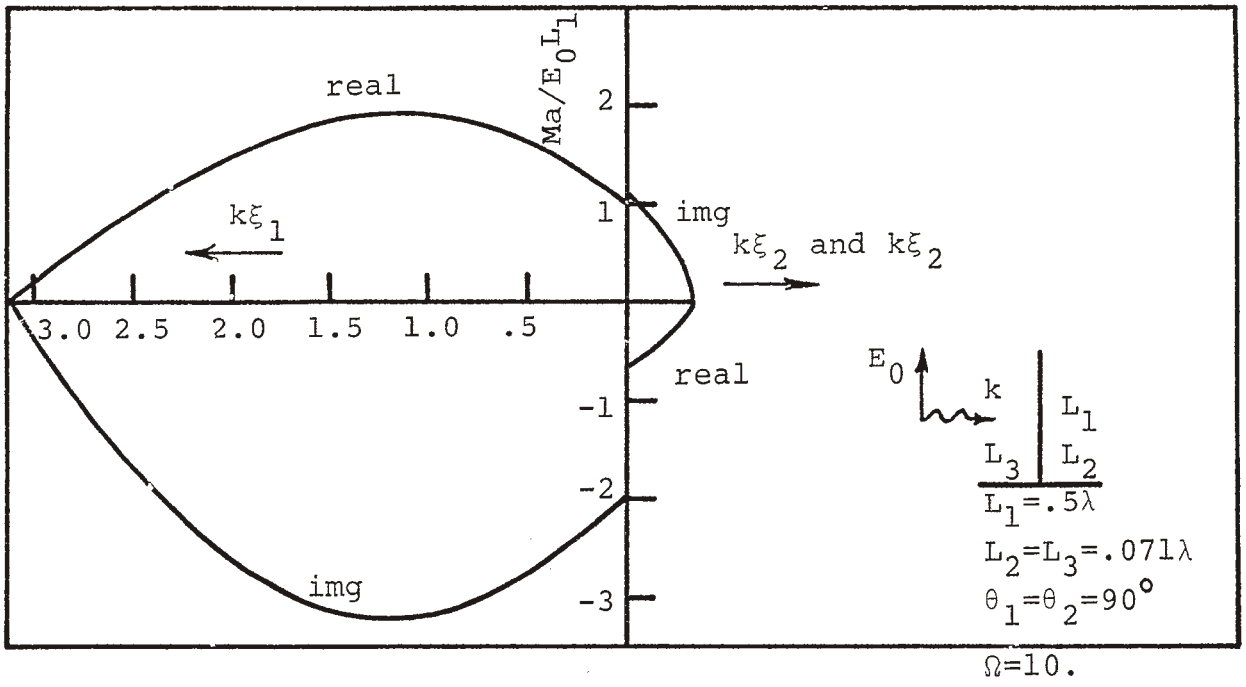

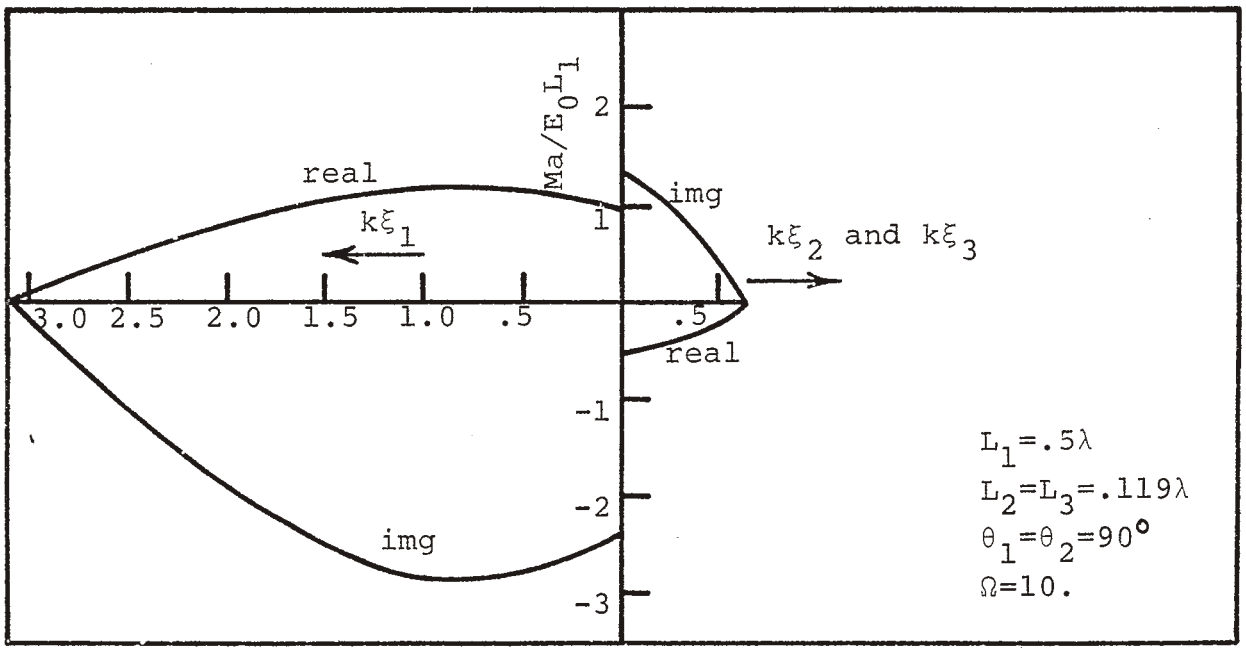

Figure 12. Plots of currents induced on inverted T structure.

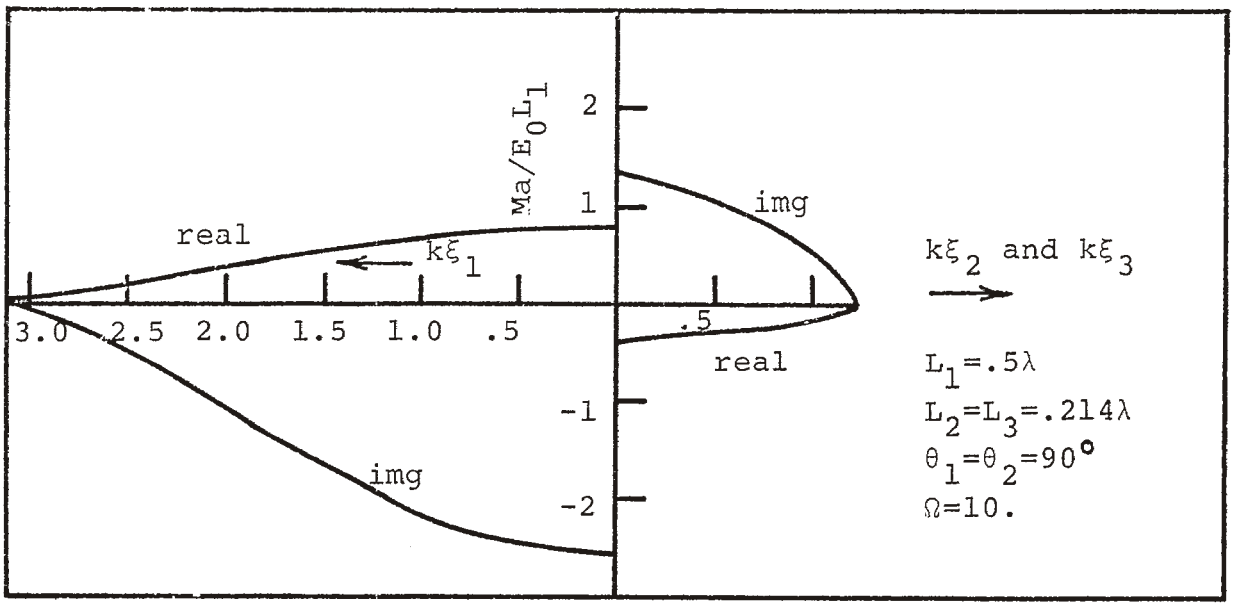

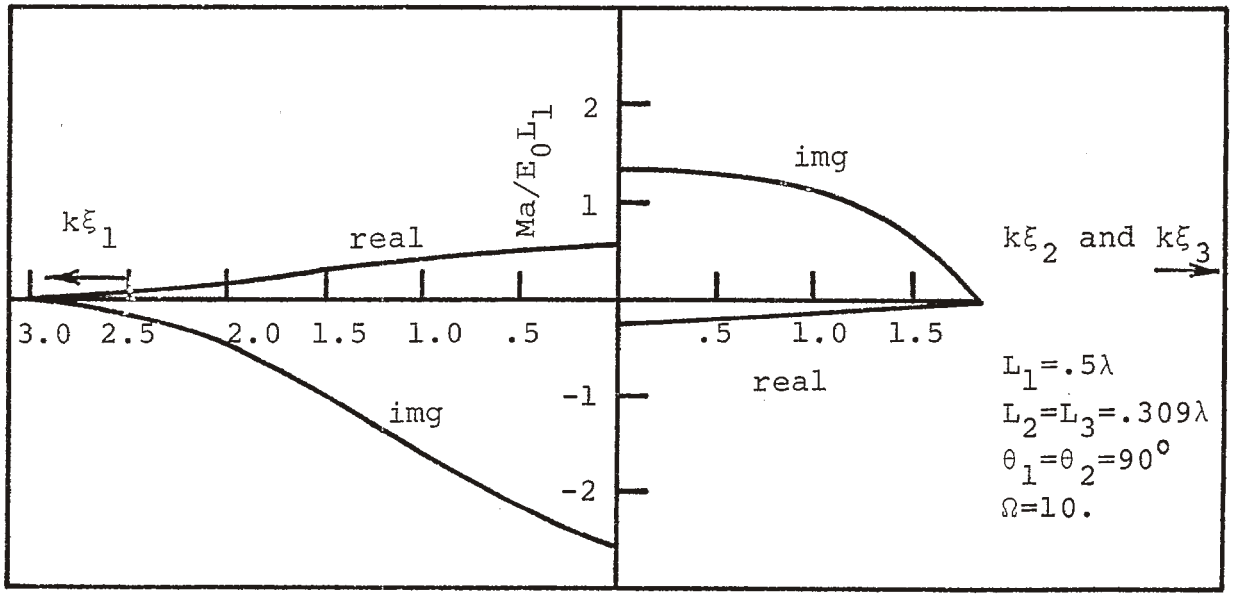

Figure 12. (con't.)

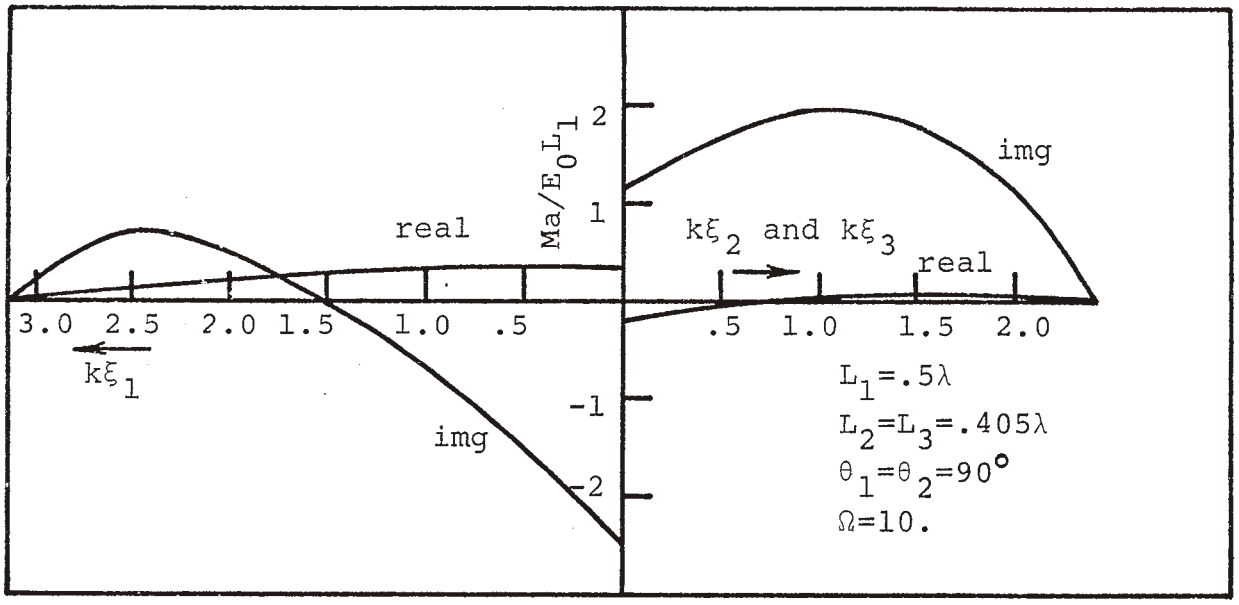

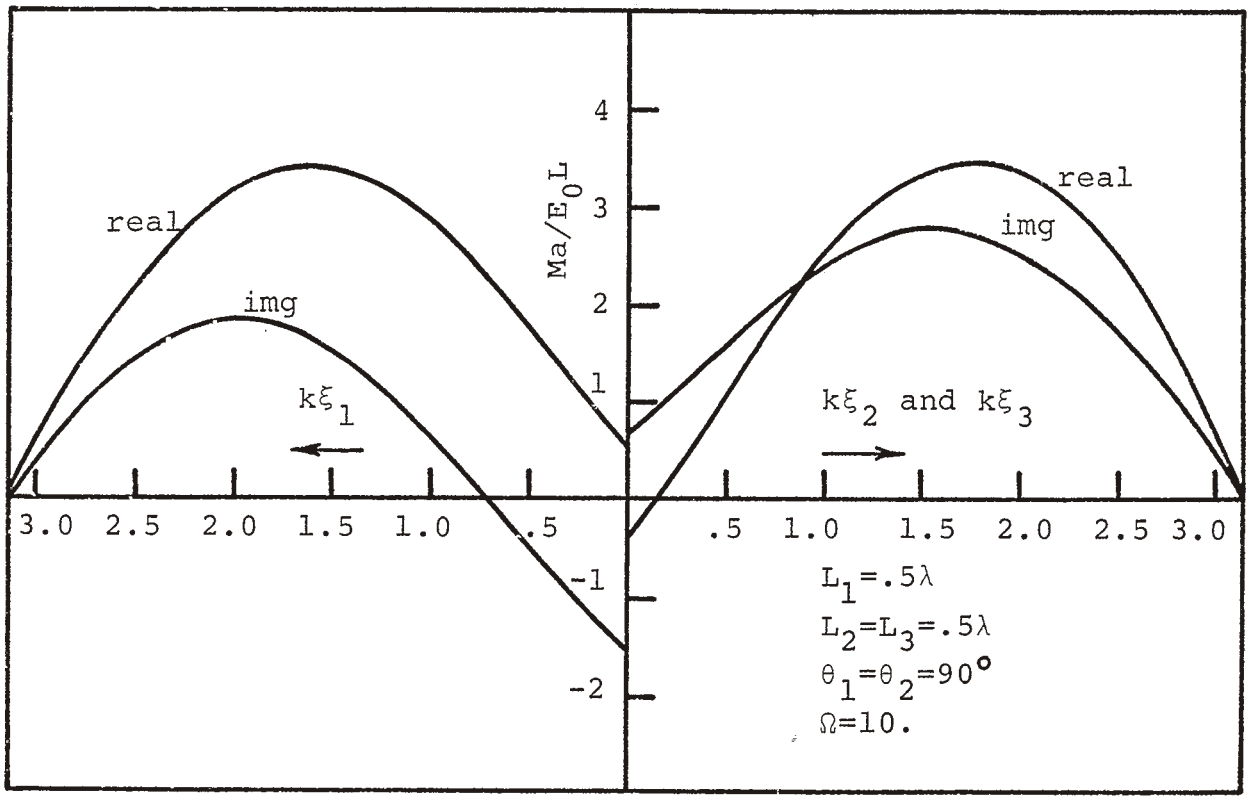

Figure 12. (cont'd.)

for the current element and directions as indicated in Figure 13. Once the $\bar{E}$ field is computed at a particular observation point, the component tangential to the wire surface can be evaluated to form the matrix element.

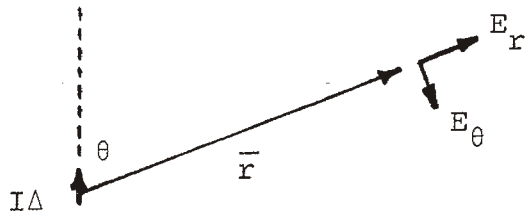

Figure 13. Electric field produced by current element $I\Delta$.

This method has been used successfully in another problem[16] but it did not involve wire junctions. Preliminary work for this junction structure involved using finite difference operators for all matrix elements for which both the source and observation points were on the same wire and the closed form expression for Z_{ij} otherwise. The results were very inaccurate and were traced to the fact that if a source point were located in the first cell of a junction, and the observation point located in one cell on either side, one matrix element would be computed by finite differences and the other by the closed form method, leading to substantial differences. Figure 14 shows this pictorially for two straight wires meeting at a junction.

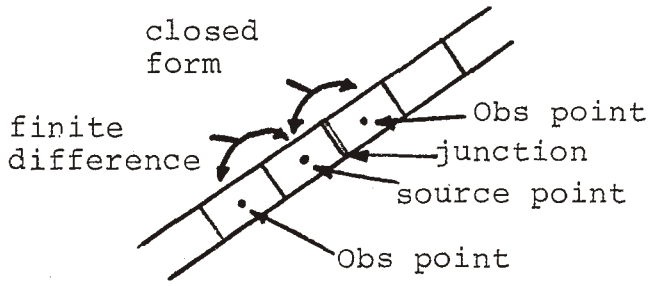

Figure 14. Source point and two adjacent observation points near the junction.

Similarly distressing results were obtained by using finite difference equations for the whole structure, but by using the surface integrated kernel[19] for the "self" terms in the matrix and using the thin-wire kernel for the crossed terms. Again, it was found that consistency in how the matrix elements are calculated as one moves through the junction point is important. Figure 15 shows, as an example of what can go wrong, the junction current on the L_1 arm as a function of the number of zones. For this structure, $L_1 = L_2 = L_3 = .25\lambda$, $\theta_1 = 90^\circ$, $\theta_2 = 120^\circ$, $\Omega = 10$. The solid lines represent the current for the case when the thin-wire kernel is employed consistently, both for the self and the crossed matrix elements. The dashed line is for the mixture of "exact" kernel and the thin-wire kernel and shows a marked degradation in accuracy of the imaginary part as the cell size decreases.

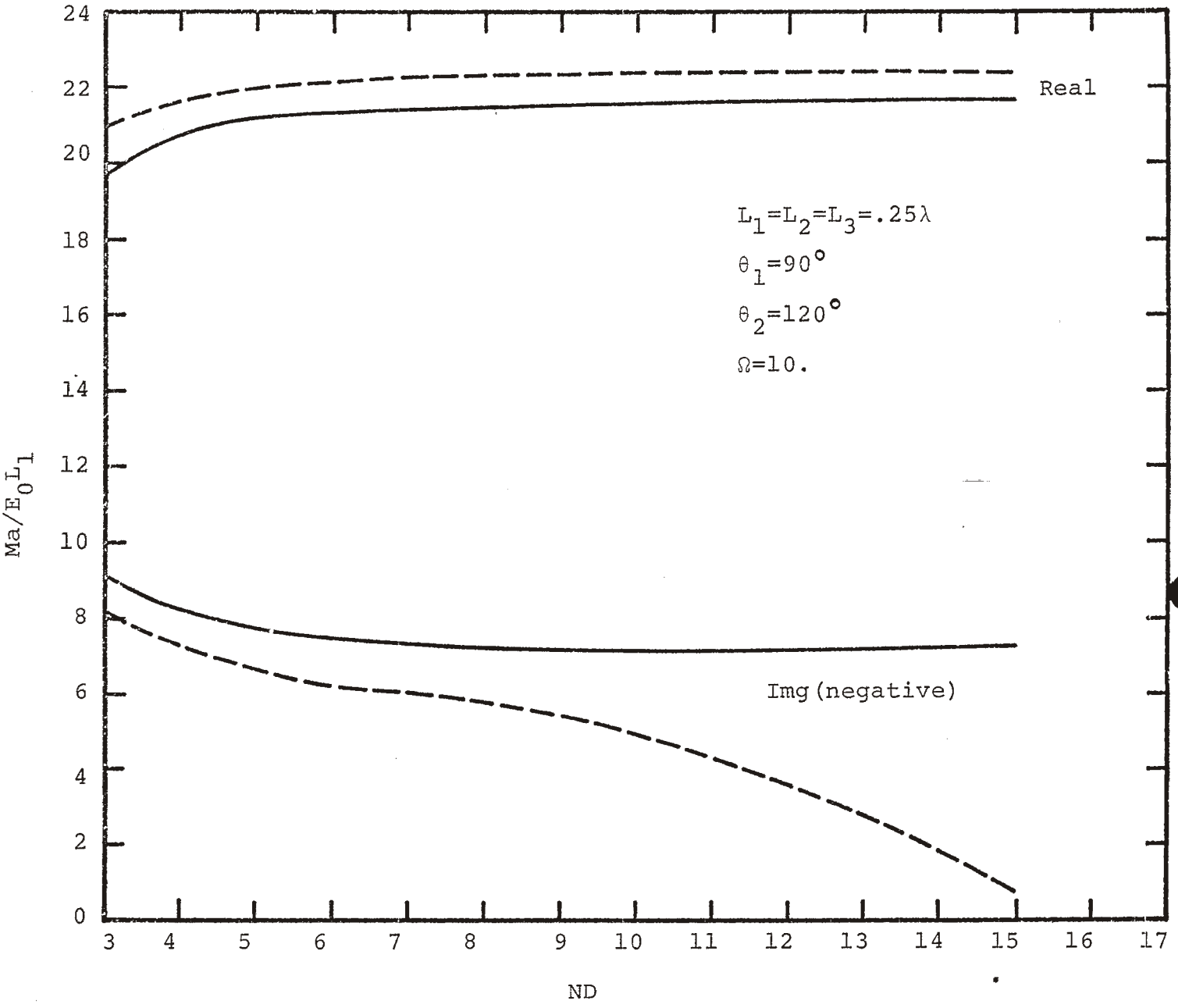

Figure 15. Plots of the junction current on the L_1 arm as a function of the number of sample points ND. Solid lines are for the consistent treatment of the kernel, dotted lines for mixed kernel.

V. Summary and Conclusions

Using the Pocklington E-field integro-differential equation, the behavior currents on three intersecting wires illuminated by a plane electromagnetic wave has been computed. Unlike other formulations, it is not necessary to use additional conditions or contraints on the currents to obtain the numerical solution as Kirchoff's current law and the condition of continuity of the charge is inherent in the integral equation. Once the numerical solution for the currents is obtained, the degree to which the junction conditions are satisifed is an indication of the overall accuracy of the numerical solution.

From the preceeding data and discussions, it is possible to draw a number of conclusions regarding the use of Pocklington's equation for intersecting wires. These may be summarized as follows:

1) As in the single thin-wire case, good numerical convergence of the current is obtained using pulse expansion functions and point matching for as few as five zones per half wavelength.

2) The interpolation or extrapolation of computed current values into other regions on the wire leads to larger errors for fewer numbers of sample points. Thus, the calculation of the input current at a junction by these methods may yield large errors if the current is not known at these points.

3) Even though the continuity of charge and Kirchoff's current law are not required as additional constraints for the numerical solution, they may be employed in interpolating the known currents to give a value for the junction currents. This results in the ability to use fewer sample points and unknowns in the numerical solution than would be normally required.

4) It is important to maintain a consistent treatment of the kernel of the integral equation, both in terms of the numerical integration and differentiation of the free space Green's function, and in relation to the type of kernel used (thin wire, surface integral, etc.). Although this is probably not very important for source and observation points well separated, it is very important for both located near the junction.

5) It is generally conceded that the Pocklington formulation will take less computer time than the Hallén formulation for arbitrary wire structures (although no data were presented here to confirm this).

The main uncertainty at the moment seems to be in understanding how to treat the intersection of thicker wires where the zone size approaches the size of the wire radius. In this case there is not only a substantial overlapping of adjacent junction zones, as shown in Figure 5, but a severe departure from the assumed condition of axially symmetric currents right at the junction. As in the case of obtaining a quasi-static correction term for the end-cap

effects of thick wires, it may be possible to determine a similar correction for junctions whose size is appreciable.

VI. References

1. Baum, C.E., "On the Singularity Expansion Method for the Solution of Electromagnetic Interaction Problems", EMP Interaction Notes, Note 88, Dec. 1971.

2. Brigham, E.O. and R.E. Morrow, "The Fast Fourier Transform", IEEE Spectrum, Vol. 4, pp. 63-70, Dec. 1967.

3. Butler, C.M., "Integral Equations for Currents Induced on a Wire Model of a Parked Aircraft", EMP Interaction Notes, Note 139, Jan. 1972.

4. Butler, C.M. and M.G. Harrison, "Numerical Solutions of Integral Equations for Currents Induced on a Wire Model of a Parked Aircraft", EMP Interaction Notes, Note 140, May 1972.

5. Chao, H.H. and B.D. Strait, "Radiation and Scattering by Configurations of Bent Wires with Junctions", IEEE Trans. A.P., Vol. AP-19, No. 5, Sept. 1971.

6. Crow, T.T. and T.H. Shumpert, "Electromagnetic Scattering from Configurations of Thin Wires with Multiple Junctions", EMP Interaction Notes, Note 99, March 1972.

7. Crow, T.T. and T.H. Shumpert, "Induced Electric Currents on Some Configurations of Wires. Part II, Non-Perpendicular Intersecting Wires", EMP Interaction Notes, Note 100, April 1972.

8. Harrington, R.F., Time Harmonic Electromagnetic Fields, McGraw-Hill, 1961.

9. Harrington, R.F., Field Computation by Moment Methods, McMillan, 1968.

10. Mei, K.K., "On the Integral Equations of Thin-Wire Antennas", IEEE Trans. A.P., Vol. AP-13, No. 3, pp. 374-378, May 1965. (Also personal communication.)

11. Miller, E.K., et al., "A Numerical Method for Obtaining the Current and Charge Distributions, and Near- and Far-Fields of Thin Wire Structures", EMP Interaction Notes, Note 84, July 1971.

12. Sancer, M.I. and A.D. Varvatsis, "Calculation of the Induced Surface Current Density on a Perfectly Conducting Body of Revolution", EMP Interaction Notes, Note 101, April 1972.

13. Shumpert, T.S. and T.T. Crow, "Induced Electric Currents on Configurations of Thick Wires: Perpendicular Crossed Wires", EMP Interaction Notes, Note 103, May 1972.

14. Taylor, C.D., Shiow-meei Lin, and H.V. McAdams, "Electromagnetic Scattering from Arbitrary Configurations of Wires", EMP Interaction Notes, Note 42, Nov. 1968.

15. Taylor, C.D. and T.T. Crow, "Induced Electric Currents on Some Configurations of Wires, Part I. Perpendicular Crossed Wires", EMP Interaction Notes, Note 85, Nov. 1971.

16. Tesche, F.M., "Numerical Determination of the Step Wave Response of a Thin-Wire Scattering Element Arbitrarily Located above a Perfectly Conducting Ground Plane", EMP Sensor and Simulation Notes, Note 141, Feb. 1972.

17. Tesche, F.M., "On the Singularity Expansion Method as Applied to Electromagnetic Scattering from Thin Wires', EMP Interaction Notes, Note 102, April 1972.

18. Tesche, F.M., "Transient Behavior of EMP Induced Currents on a Sphere with a Trailing Wire Antenna. Part I, Formulation of the Integral Equation", EMP Interaction Notes, Note 137, April 1973.

19. Tesche, F.M., "Evaluation of the Surface Integral Occurring in the E-Field Integral Equations for Wire Antennas", ACT Mathematics Notes, Note 29, Sept. 1973.

20. Van Bladel, J., Electromagnetic Fields, McGraw Hill, 1964.

21. Van Bladel, J., "Some Remarks on Green's Dyadic for Infinite Space", IRE Trans. A.P., Vol. 9, pp. 563-566, 1961.